Geophys. J. Int. (1995) **121,** 789–804

Spreading-rate-dependent magnetization of the oceanic lithosphere inferred from the anomalous skewness of marine magnetic anomalies

J. Dyment* and J. Arkani-Hamed

Earth and Planetary Sciences, McGill University, 3450 University, Montréal, Québec H3A-2A7, *Canada*

Accepted 1994 December 2. Received 1994 November 21; in original form 1994 August 1

SUMMARY

The anomalous skewness of marine magnetic anomalies decreases with increasing spreading rate and becomes negligible above a spreading rate of about 50 km Myr^{-1}. Previous magnetization models of the oceanic lithosphere fail to explain this observation. We propose a new model in which the magnetic structure of the oceanic lithosphere is dependent on spreading rate. Anomalous skewness measurements for anomalies 33 reversed and 25 reversed at various spreading rates are in agreement with a magnetization model in which layer 3 and the uppermost mantle bear a similar saturation magnetization, and the ratio of layer 3 over layer 2A saturation magnetizations varies linearly from about 0.4 at a spreading rate of 10 km Myr^{-1} to about 0 at 55 km Myr^{-1}. For spreading rates higher than 55 km Myr^{-1}, layer 3 and uppermost mantle magnetizations are negligible. Recent advances concerning accretionary processes at mid-ocean ridges suggest that the combined effect of variations with spreading rate of magma fractionation, alteration of layer 2A, and serpentinization of layer 3 and the uppermost mantle may account for the proposed variation of magnetization with spreading rate.

Key words: anomalous skewness, magnetic anomalies, mid-ocean ridge processes, spreading rate.

INTRODUCTION

The phase, or skewness, of sea-floor spreading marine magnetic anomalies primarily depends on the inclination of the magnetization and geomagnetic field vectors. However, skewness analysis of magnetic anomalies from a worldwide distribution of conjugate basins has demonstrated the existence of a residual component, the anomalous skewness (e.g. Cande 1976; Cande & Kristoffersen 1977; Cande 1978; Roest, Arkani-Hamed & Verhoef 1992; Dyment, Cande & Arkani-Hamed 1994). This arises because the conventional oceanic crustal magnetization model i.e. the rectangular 2-D layer 2A prisms of constant magnetization with alternating polarity, is only a first-order representation and does not account for the details of the marine magnetic anomalies. Several models have been proposed to explain the anomalous skewness of marine magnetic anomalies. They include temporal variations of the geomagnetic field intensity within a given polarity period, tectonic rotation of the source layer, acquisition of a secondary magnetization in the upper crustal layer 2A, and magnetization of the deep crust and uppermost mantle controlled by the thermal structure of the oceanic lithosphere.

In this paper, we examine these models in the light of recent results on the anomalous skewness and its relationship with spreading rate obtained from the analyses of marine magnetic anomalies in the Atlantic and Indian Oceans (Roest *et al.* 1992; Dyment *et al.* 1994). Our investigations are limited to the Late Cretaceous and Cenozoic marine magnetic anomalies, and do not include the Mesozoic anomalies which have very small or no anomalous skewness (Cande & Kristoffersen 1977; Cande & Kent 1985; Roest *et al.* 1992). The Mesozoic anomalies pre-date the long, normal geomagnetic polarity period of the Cretaceous Quiet Zone, and their magnetic sources have probably been affected during this period (Arkani-Hamed 1989, 1991). We show that the existing models do not account for the relationship between anomalous skewness and spreading rate, and propose a new model, based on spreading-rate-dependent thermo-viscous remanent magnetization of the oceanic crust and uppermost mantle, which successfully explains the characteristics of the anomalous skewness and takes into account petrological and geochemical variations of the oceanic lithosphere.

EXISTING ANOMALOUS SKEWNESS MODELS

The anomalous skewness measured on real magnetic anomaly data decreases with increasing spreading rate and

* Also at: URA 1278 et GDR GEDO, Université de Bretagne Occidentale, BP 809, 6 Avenue Le Gorgeu, 29285 Brest Cedex, France.

becomes negligible above 50 km Myr^{-1} (Roest *et al.* 1992; Dyment *et al.* 1994; Fig. 1). At a given spreading rate, the anomalous skewness is also different for different anomalies (e.g. Roest *et al.* 1992; Fig. 1), an observation related to the effect of unevenly distributed neighbouring magnetic sources on the skewness of these anomalies (Dyment *et al.* 1994). Among the available anomalous skewness measurements, we selected those of anomalies 33 reversed (33r) and 25 reversed (25r), because they span the widest range of spreading rates. Both series of measurements define a trend similar to the general relationship between anomalous skewness and spreading rate, anomaly 33r showing high anomalous skewnesses and anomaly 25r medium anomalous skewnesses (Fig. 1). In this section, these observations are compared with the anomalous skewnesses of the synthetic anomalies 33r and 25r produced by different existing models. The various methods that have been proposed to measure anomalous skewness lead to results similar within the confidence interval on the measurements (see Dyment *et al.* 1994 for a review). We apply the visual method used by Dyment *et al.* (1994) to determine the anomalous skewness of the synthetic magnetic anomalies computed at the geomagnetic pole.

Temporal variation of the geomagnetic field

Cande (1978) proposed two types of geomagnetic field temporal variations that could give rise to the anomalous skewness: the increasing occurrence of short, opposite polarity episodes before a reversal, and a gradual decay of geomagnetic field intensity within a polarity interval. Short episodes of intensity variations of the marine magnetic anomalies inside a given polarity interval, the 'tiny wiggles', have been observed in the fast-spreading oceanic areas (Cande & LaBrecque 1974; Cande & Kent 1992). They are recognized within anomalies 5–6 (Blakely 1974; Cande & LaBrecque 1974), anomalies 12–13 (Cande & LaBrecque, 1974), and anomalies 24–27 (Cande & Kent 1992), but are probably present in the entire geomagnetic polarity time-scale. These short events appear to be totally random and do not exhibit any increasing occurrence prior to the main polarity reversals (Cande & Kent 1992). Therefore they do not seem to be the cause of anomalous skewness.

Cande (1978) noted that the gradual decay of geomagnetic intensity contradicts the conventional model of the geomagntic field reversal as generated by a stochastic process (Cox 1969; Phillips, Blakely & Cox 1975; Phillips & Cox 1976). The gradual decay requires the core to have a memory longer than 1 Myr, whereas the conventional model predicts no more than 0.01 Myr memory (Cox 1975). Whether such a gradual decay is supported by the sedimentary palaeointensity records of the geomagnetic field is a matter of controversy. Although reliable data are sparse, some continuous sedimentary records of the Brunhes, Matuyama and anomaly 12r chrons do not present any consistent pattern within a polarity interval (Tauxe 1993), while some other records spanning the last 4 Ma indicate a systematic decay of the field within each polarity period (Valet & Meynadier 1993).

To test the gradual decay model, magnetic anomalies were computed under the assumption of rectangular, 2-D layer 2A prisms with alternating polarity and exponentially decaying magnetization within a polarity interval, as suggested by Cande (1978). Different characteristic times for

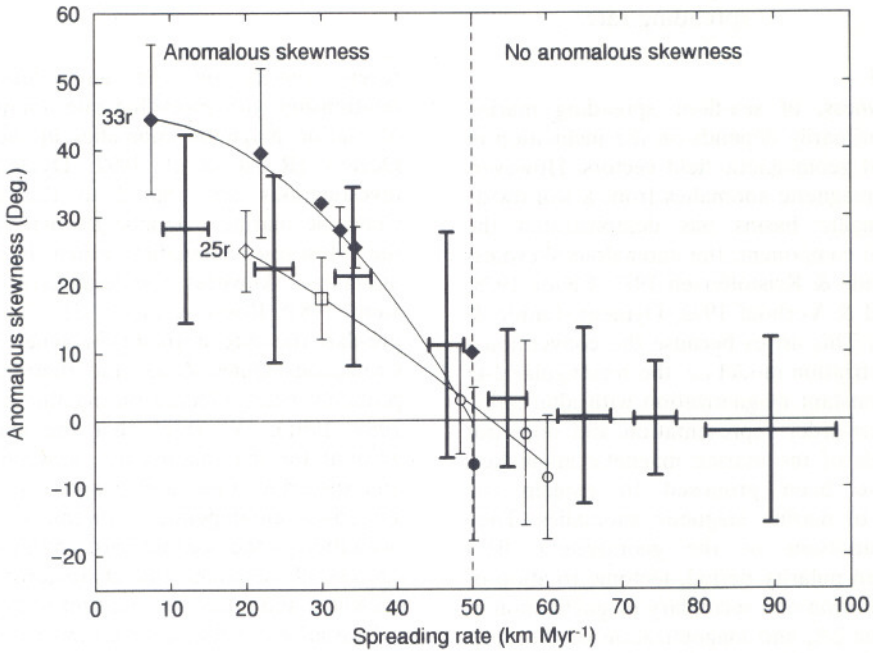

Figure 1. Anomalous skewness versus spreading rate: observations. Bold uncertainty bars show averages and standard deviations, within 10 km Myr^{-1} intervals (20 km Myr^{-1} intervals below 20 km Myr^{-1} and above 80 km Myr^{-1}) of the available skewness determinations for all anomalies (Dyment *et al.* 1994). There is a limit at a spreading rate of 50 km Myr^{-1} (dotted line) below which a significant anomalous skewness is observed and above which anomalous skewness is negligible. Black symbols are anomalous skewness determinations for anomaly 33 reversed (33r), white symbols for anomaly 25r. The square is from Petronotis, Gordon & Acton (1989), diamonds are from Roest *et al.* (1992), and circles are from Dyment *et al.* (1994).

decay (0.5–5 Myr) and spreading rates (10–70 km Myr^{-1}) were used. Fig. 2(a) shows that the model does not account for the relationship between anomalous skewness and spreading rate, although the anomalous skewness predicted by the exponential decay model generally decreases with faster spreading rate.

Crustal tectonic rotation

The outward tectonic rotation of magnetized crustal blocks modifies the inclination of the magnetization vector and can be a plausible cause for the anomalous skewness (Cande 1978; Verosub & Moores 1981). Faulting of the crust increases with lower spreading rates and suggests that tectonic rotation may account for the observed relationship between anomalous skewness and spreading rate. Because 1° of rotation results in 1° of anomalous skewness, Cande (1978) remarked that the 40° anomalous skewness observed in the North Atlantic for anomalies 33–34 requires a 40° tectonic rotation. In the case of tilted blocks, such a rotation implies faults dipping at 40°, a value much larger than the 10° generally observed (Cande 1978). Tectonic rotations may occur along listric faults, as suggested by Verosub & Moores (1981) to explain palaeomagnetic observations on Deep Sea Drilling Project data. However, the predicted 58° rotation at site 417 disagrees with the negligible anomalous skewness observed on anomalies M0–M4 in the vicinity of the site (Cande & Kent 1985). Simple geometrical considerations show that the tectonic rotation model is inadequate to explain the large anomalous skewnesses, 30°–45°, observed at slow and intermediate spreading centres. This is because (a) layer 2A, which is probably the

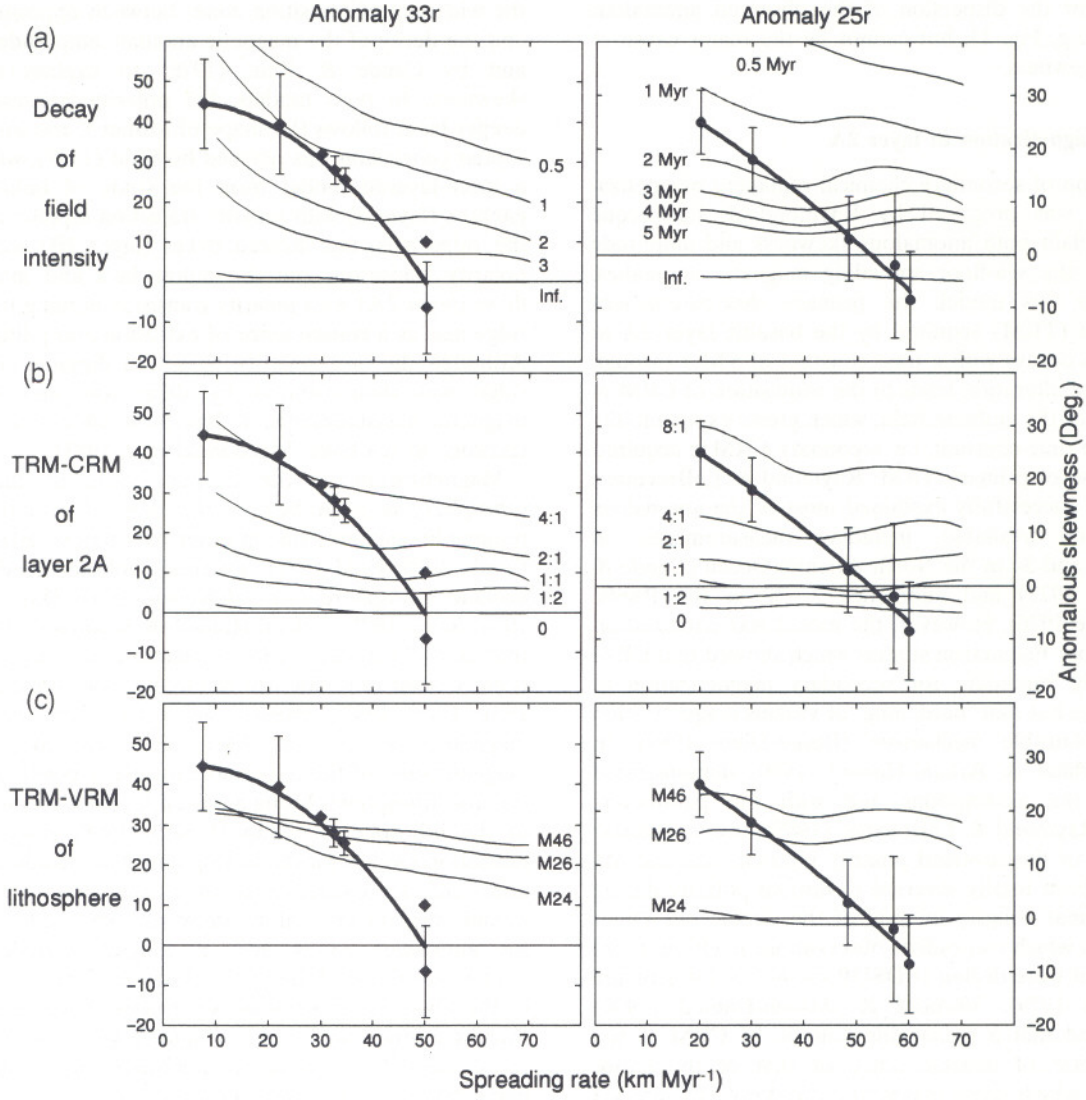

Figure 2. Anomalous skewness versus spreading rate: predictions of existing models. Diamonds (anomaly 33r) and circles (anomaly 25r), error bars and thick lines display observations, whereas thin lines show the anomalous skewness measured on synthetic magnetic anomaly profiles computed at the pole under the assumption of the various models. (a) Gradual decay of the geomagnetic field intensity. The numbers denote the decay time. (b) TRM and CRM model of Raymond & LaBrecque (1987) for layer 2A. The numbers denote the CRM : TRM ratio. (c) TRM and VRM model of Arkani-Hamed (1989) for the crust and the uppermost mantle. M24, M26 and M46 refer to the blocking temperature ranges and relative amounts of layer 2A, layer 3 and uppermost mantle magnetizations proposed by Arkani-Hamed (1989).

major contributor to the marine magnetic anomalies, is less than 1 km thick, (b) this layer has to be more or less continuous horizontally to generate recognizable magnetic anomalies, and (c) the observed anomalous skewnesses of 45° (at slow spreading centres) or 30° (at intermediate spreading centres) imply major faults at about every kilometre, in contradiction with the width of faulted blocks observed on the slow Mid-Atlantic Ridge at 37°N (6–12 km, Macdonald & Luyendyk 1977) and on the intermediate East Pacific Rise at 21° (5–10 km, Macdonald & Loyendyk 1985) and the South-east Indian Ridge at 27°41′S (8 km, Sauter *et al.* 1991). In addition, the significant population of outward-facing faults observed at slow and intermediate spreading centres probably reduces the effect of outward tectonic rotation (along the opposite inward-facing faults) on the anomalous skewness. These geometrical considerations suggest that the tectonic rotation can locally account for 5° to 10° of the anomalous skewness and may be partly responsible for the dispersion of the observed anomalous skewnesses (e.g. Fig. 1), but cannot be the major cause of anomalous skewness.

Secondary magnetization of layer 2A

The acquisition of secondary chemical remanent magnetization (CRM) was proposed by Raymond & LaBrecque (1987) to explain both anomalous skewness and amplitude variations of the sea-floor spreading magnetic anomalies. According to this model, the primary thermoremanent magnetization (TRM) acquired by the basaltic layer 2A at the ridge axis decays with a time constant of 5 Myr through alteration. The alteration leads to the acquisition of CRM in the direction of the ambient field, which grows exponentially with the same time constant, i.e. secondary CRM is acquired at the expense of primary TRM. Raymond & LaBrecque's (1987) model successfully explained most of the anomalous skewness then available, including measurements on anomalies 33 and 34 in the North Atlantic Ocean (Cande & Kristoffersen 1977) and anomalies 27–32 in the Pacific Ocean (Cande 1976). However, the model was criticized on the basis of rock magnetism studies which showed that CRM is an unlikely candidate for secondary magnetization in oceanic basalts but that 'hardening' of viscous magnetization is a more plausible mechanism (Beske-Diehl 1989). In addition, Verhoef & Arkani-Hamed (1990) demonstrated that, under the assumptions and with the parameters choosen by Raymond & LaBrecque (1987), the magnetization of rocks of the reversed polarity intervals M0 and M1 should have been totally inverted to normal polarity during the long, normal polarity interval of the Cretaceous Quiet Zone, a result which contradicts observations made on rocks of this age that were drilled at DSDP site 417 in the Atlantic Ocean (Levi 1979). Verhoef & Arkani-Hamed (1990) further showed that a reasonable amount of CRM of the upper kilometre of oceanic crust, or that of the entire oceanic crust, which keeps magnetization of polarity interval M0 reversed, fails to explain the observed anomalous skewness.

We have examined Raymond & LaBrecque's (1987) model by calculating magnetic anomalies for different CRM : TRM ratios (4 : 1–1 : 2) and spreading rates (10–70 km Myr^{-1}). Fig. 2(b) shows the result for anomalies 33r and 25r together with the observed anomalous skewness. The anomalous skewness predicted for anomaly 33r assuming a CRM : TRM ratio of 4 : 1 agrees reasonably well with the observations for spreading rates lower than 30 km Myr^{-1}; for faster spreading rates, however, the model does not agree with the observations. For anomaly 25r, the Raymond & LaBrecque (1987) model predicts a roughly constant anomalous skewness for spreading rates ranging between 10 and 70 km Myr^{-1}, thus failing to explain the observations.

Primary and secondary magnetizations of the oceanic lithosphere

The previous models considered magnetization of only the upper crustal layer 2A, which is about 0.5 to 1 km thick. Alternative models incorporating a contribution of deeper crustal layers were proposed by Blakely (1976) to explain the widening of transition zones between opposite polaritys and the decay of the magnetic anomaly amplitude with age, and by Cande & Kent (1976) to explain anomalous skewness. In both models, the polarity transition of the deeper layer follows the shape of former Curie isotherms. A similar conclusion was reached by Kidd (1977), who derived a three-layered model from the study of ophiolites, the gabbros (layer 3) with polarity transition dipping away from the ridge axis, the sheeted dykes (layer 2B) with vertical polarity transition, and the pillow lava and massive lava flows (layer 2A) with polarity transition dipping towards the ridge axis as a consequence of extrusion and piling of flows. Although the lava polarity transition dipping towards the ridge was demonstrated by deep tow and submarine magnetic measurements, it has little effect on anomalies recorded at sea-level (Macdonald *et al.* 1983).

Magnetization of the deeper layers of the oceanic lithosphere is controlled by the thermal evolution of the oceanic lithosphere, among other parameters (Blakely 1976; Cande 1976; Kidd 1977). Thermal evolution models of the oceanic lithosphere (e.g. McKenzie 1969; Davis & Lister 1974; Sleep 1975; Arkani-Hamed & Strangway 1987) show that a 6–7 km deep Moho, characteristic of a 'normal' oceanic crust (e.g. Spudich & Orcutt 1980; Reid & Jackson 1981; Chen 1992), crosses the 600 °C Curie isotherm of magnetite as early as 2 Myr after creation, and that magnetization of the uppermost mantle is possible for older oceanic lithosphere. Using a typical thermal evolution model of the lithosphere, Arkani-Hamed (1989) proposed magnetization models for the lithosphere that include both TRM and secondary viscous remanent magnetization (VRM). The models explain anomalous skewness observed at sea-level for anomalies 33–34 and at Magsat altitude for the Cretaceous Quiet Zone in the Atlantic Ocean. Comparison of the observed anomalous skewnesses at sea-level and the Magsat altitude and those computed for various spreading rates, magnetic blocking temperature ranges and relative magnetization of the upper crust, lower crust and uppermost mantle shows that the anomalous skewness of marine magnetic anomalies is mainly controlled by the lower crustal magnetization, while that of Magsat anomalies mostly depends on the uppermost mantle magnetization (Arkani-Hamed 1989, 1991). The TRM–VRM model has also proved successful in explaining anomalous skewness of anomaly 33r

off the coast of Newfoundland, and partially accounts for the long-wavelength negative magnetic anomaly observed over the Labrador Sea (Arkani-Hamed 1990).

We have examined Arkani-Hamed's (1989) model by calculating magnetic anomalies for different spreading rates (10–70 km Myr^{-1}) and magnetic blocking temperature ranges of 200–400 °C (model 24), 200–600 °C (model 26) and 400–600 °C (model 46). The magnetized zone is limited by the Curie isotherm. We assigned saturation magnetizations of 6 A m^{-1} for layer 2A (all models); 0 A m^{-1} for layer 2B (all models); 4.2, 2.1 and 1.5 A m^{-1} for layer 3 (models 24, 26, and 46 respectively); and 1.8, 2.1 and 1.5 A m^{-1} for the uppermost mantle down to a maximum depth of 30 km (models 24, 26, and 46, respectively). The saturation magnetization represents the magnetization that would be acquired under a constant geomagnetic polarity in an infinite time. Comparison of predicted and observed anomalous skewnesses was performed for anomalies 33r and 25r (Fig. 2c). Anomalous skewness of synthetic anomalies 33r computed for models 26 and 46 agrees reasonably well with the observations for spreading rates between 30 and 40 km Myr^{-1}. For slower or faster spreading rates, however, the models do not explain the measurements. This discrepancy is further demonstrated by a similar comparison for anomaly 25r. The predicted anomalous skewness is almost constant, while the observed one shows significant variations with spreading rate.

None of the aforementioned models succeeds in explaining the observed anomalous skewness and its relationship with spreading rate. The processes involved in these models (with the exception of tectonic rotations) only modify the geomagnetic input signal as a function of time, and the crustal magnetization direction remains the same for all spreading rates. The anomalies are different for different spreading rates because of the convolution with the earth filter (Schouten & McCamy 1972), which selects a frequency band that is different for different spreading rates. The resulting phase shift changes with the frequency band and produces an apparent spreading-rate-dependent anomalous skewness. The variations with spreading rate of anomalous skewness for the synthetic magnetic anomalies 33r and 25r reflect the absence of normalization of these magnetic anomalies to a given spreading rate (Schouten & McCamy 1972; Cande 1978) for the various source models considered (Dyment *et al.* 1994). These variations are remarkably similar for the exponential decay model, the CRM model of layer 2A and the TRM–VRM model of the crust and uppermost mantle (Fig. 2). The anomalous skewness of synthetic anomaly 33r decreases with increasing spreading rate, while that of synthetic anomaly 25r remains roughly constant. Even the second-order variations that are probably related to the effect of neighbouring sources on the skewness of a given anomaly are similar for the different models.

The decrease of observed anomalous skewness with faster spreading rate is significantly greater than that predicted by the above models. This shows that the spreading-rate dependence of anomalous skewness survives normalization of the original magnetic anomaly data to a given spreading rate, and strongly suggests a spreading-rate-dependent magnetization in order to explain the observed anomalous skewness. Obviously, the models involving variations of the geomagnetic field intensity should be discarded because the dynamic characteristics of the outer core may not directly correlate with the sea-floor spreading velocities. The faulting of the crust and block rotations are probably spreading-rate-dependent, but cannot account for the observed anomalous skewness. Even if the acquisition of CRM in layer 2A is a spreading-rate-dependent process, the contradiction noted by Verhoef & Arkani-Hamed (1990) cannot be reconciled: the observed anomalous skewness for anomaly 33r requires a CRM : TRM ratio equal to 4 : 1 at a slow spreading rate, which is incompatible with the reverse magnetization observed at DSDP site 417 in the oceanic crust created at anomaly M0 time at a slow spreading centre (Levi 1979). The maximum CRM : TRM ratio that prevents the reversal of magnetization created at anomaly M0 time is 1 : 2 and it generates only about 10° of anomalous skewness (Verhoef & Arkani-Hamed 1990). The anomalous skewness predicted by the TRM–VRM model of the oceanic lithosphere arises from the combination of two magnetic sources: layer 2A, which is essentially made of rectangular prisms of constant magnetization and produces almost no anomalous skewness, and the lower crust and uppermost mantle, which produce a very strong anomalous skewness. The amount of anomalous skewness predicted by this model is a direct consequence of the relative magnetization of these different sources, which can be modified to take into account the variations of the oceanic lithosphere with spreading rate.

A SPREADING-RATE-DEPENDENT MAGNETIC STRUCTURE OF THE OCEANIC LITHOSPHERE

In this section, we review results from rock magnetism and long-wavelength magnetic anomaly studies, which suggest a significant magnetization of the oceanic lower crust and uppermost mantle. We also review recent developments in accretionary processes at mid-oceanic ridges in order to investigate the possible mechanism(s) that may account for a spreading-rate-dependent magnetization of the oceanic lithosphere.

Magnetization of the lower crust and uppermost mantle

Strong evidence for a significant magnetization of the oceanic lower crust comes from numerous rock magnetism studies. Harrison (1976, 1981) remarked that the magnetization measured on basalts recovered by the Deep Sea Drilling Project is too small to account for the magnetic anomalies, and proposed that layer 3 bears a significant magnetization. Such a contribution was measured on rock samples by various authors and reaches about 0.5 to 1 A m^{-1} for layer 3 (Kent *et al.* 1978; Dunlop & Prévot 1982; Banerjee 1984; Harrison 1987) and as much as 5 A m^{-1} for basal serpentinized peridotites (Harrison 1987). In addition, recent data from ODP Hole 735B suggest that layer 3 rocks are capable of recording reversals of the Earth's magnetic field (Pariso & Johnson 1993a), emphasizing that the gabbros are important contributors to magnetic anomalies of the oceanic crust (Pariso & Johnson 1993b). However, there is no agreement on the magnetization of layer 2B. Many authors consider magnetization of this layer as negligible

(Kent *et al.* 1978; Dunlop & Prévot 1982; Smith 1984), whereas sheeted dykes from DSDP hole 504B exhibit a high magnetization of 2 A m^{-1} (Smith 1985).

There is indirect evidence for the magnetization of the oceanic lower crust and uppermost mantle which comes from the analysis of long marine profiles (Harrison & Carle 1981) and from intermediate-wavelength magnetic anomalies derived from Magsat data. For instance, modelling of the Magsat anomaly associated with subduction zones (Arkani-Hamed & Strangway 1987), passive margins (Hayling 1991), boundaries between oceanic domains of different ages (Council, Achache & Galdeano 1989), and Cretaceous Quiet Zones (Toft & Arkani-Hamed 1992) requires a significant magnetization of the uppermost mantle. Rock magnetism studies on oceanic samples and ophiolites provide additional evidence for uppermost mantle magnetization (see references cited in Toft & Arkani-Hamed 1992).

The fresh oceanic basalt has a strong TRM at the time of formation which is probably the cause of the high-amplitude axial anomaly. However, this magnetization decreases with time as the alteration processes destroy the magnetic minerals (Macdonald 1977; Dunlop & Hale 1977; Bleil & Petersen 1983; Smith & Banerjee 1986; Woolridge *et al.* 1990). In addition to TRM, rock magnetism studies have shown that viscous magnetization is important in the deep crust and probably in the uppermost mantle (Dunlop & Hale 1977; Smith 1984; Bina & Henry 1990; Pozzi & Dubuisson 1992). Viscous magnetization acquired by a magnetic material during a given polarity interval can be removed after a polarity reversal and replaced by opposite viscous magnetization. However, because of its strong temperature dependence and since temperature decreases with time, a significant part of the viscous magnetization may not be removed but remain as VRM (e.g. Dunlop 1973, 1981).

Slow/cool and fast/hot spreading centres

Many studies of mid-oceanic ridges by various geophysical methods have shown that both the spreading rate and the thermal state of the lithosphere play a major role in spreading centre processes and the structure of the oceanic crust. Slow/cool spreading centres are associated with an axial valley, while fast/hot spreading centres exhibit an axial high (e.g. Macdonald 1982, 1986). Axial valleys gradually get shallower with increasing spreading rates, although local effects may affect this relationship (e.g. Malinverno 1993). A strong gravity anomaly is generally associated with axial valleys, while such an anomaly is subdued over fast spreading ridges (Cochran 1979). The satellite altimetry and gravity anomaly data clearly show an abrupt change in the ridge axis gravity with spreading rate occurring between 30 and 35 km Myr^{-1} (Small & Sandwell 1989). These characteristics of the spreading centre are sensitive to local variations of temperature and chemistry (Cochran 1991). The roughness of bathymetry and gravity anomaly gradually decreases with increasing spreading rate (Malinverno 1991; Small & Sandwell 1992).

By contrast, seismic refraction data show that the average crustal thickness of the 'normal' oceanic crust (i.e. away from plateaus) is always about 6 km, regardless of the spreading rate (Chen 1992). Variations around this average are, however, larger for slow (±3 km) than for fast (±1 km) spreading centres. This apparent thickness uniformity does not mean a thermomechanical uniformity, as demonstrated by the deepening and thickening of the seismogenic layer with slower spreading rates (Huang & Solomon 1988). Seismic reflection profiles across fast or intermediate spreading centres image a strong reflector beneath the ridge axis, which tends to be shallower at faster spreading rates (Purdy *et al.* 1992). The reflector is interpreted as the top of a partially molten magma chamber (Detrick *et al.* 1987; Morton & Sleep 1985; Morton *et al.* 1987). Such a reflector has not been observed at a slow spreading centre (e.g. Detrick *et al.* 1990).

Petrological and geochemical data also suggest a basic difference between slow/cool and fast/hot spreading centres. There is increasing evidence that gabbro and serpentinized peridotite outcrops are rather common on slow/cool spreading centres, while they are rarely observed on fast/hot spreading centres (e.g. Cannat 1993). Major elements of mid-ocean ridge basalts collected at fast spreading centres (>30 km Myr^{-1}) exhibit the so-called 'global trend' (Klein & Langmuir 1989), which corresponds to a positive correlation between the extent of melting and pressure, while those of slow spreading centres (<25 km Myr^{-1}) present the opposite 'local trend' (Niu & Batiza 1993). This arises from fundamental differences in the dynamics of mantle upwelling and melt segregation beneath slow and fast spreading ridges. The 'global trend' corresponds to 2-D passive mantle upwelling in response to plate separation, while the 'local trend' is consistent with 3-D buoyant mantle diapirism (Parmentier & Phipps Morgan 1990).

Slow/cool spreading centres are associated with very short-lived or non-existing partially molten magma chambers and are dominated by tectonic and intrusive processes which result in a complex structure of the crust. Fast/hot spreading centres are associated with permanent or long-lived partially molten magma chambers and are dominated by magmatic processes which result in a simpler structure of the crust, as shown by smoother bathymetry and gravity anomaly. Hydrothermal cooling, mantle temperature and crustal thickness also play an essential role in the thermal evolution and the rheological properties of the oceanic lithosphere, and therefore in the spreading rate at which the transition occurs between slow and fast spreading centres.

Spreading-rate-dependent magnetization

Which process(es) may lead to variations of magnetization in the oceanic lithosphere with spreading rate? The variations may arise from differences in the rocks emplaced at slow and fast spreading centres, or from a different later evolution, for instance alteration of basalts and reduction of their magnetization and/or serpentinization of peridotite and acquisition of additional magnetization. A major difference between fast and slow spreading centres is the presence or absence of a partially molten magma chamber beneath the ridge axis, which is strongly related to the degree of melting and fractionation of the upper mantle, and thus to the amount of Mg/Fe of the erupted basaltic rocks (layer 2A). The presence of a magma chamber implies a

higher degree of fractionation, and therefore a lower Mg/Fe content of layer 2A (Sinton & Detrick 1992). Indeed, the layer 2A content of iron oxides increases with increasing spreading rates (Niu & Batiza 1993). Although the consequences of such a relationship on the amount of titanomagnetite in erupted basalts is complex, rock magnetic measurements of oceanic basalt suggest that a higher degree of fractionation is associated with an increase in the concentration of titanomagnetite and, therefore, with a higher magnetization of layer 2A (Sempere 1991). This indicates higher layer 2A magnetization for the fast spreading centres.

Alteration by hydrothermal circulation within a newly formed oceanic crust is an essential process, as indicated by the decay of magnetic anomaly amplitude (e.g. Macdonald 1977; Wittpenn, Harrison & Handschumacher 1989; Geiss, Petersen & Bleil 1989; Sayanagi & Tamaki 1992), by the decrease of magnetization intensity of oceanic rocks (Dunlop & Hale 1977; Bleil & Petersen 1983; Woodridge *et al.* 1990; Johnson & Pariso 1993; Furuta 1993), by the decrease in seismic velocities of layer 2 (Christensen & Salisbury 1972) and by the heat flux variations (Stein & Stein 1994) with age. Since tectonics play a major role at slow spreading centres, while magmatism dominates fast spreading centres, it is expected that the oceanic basaltic layer is more pervasively fractured at slow than at fast spreading centres. In addition, the basaltic layer 2A may be thinner at slow/cool (low magma supply) spreading centres (Cannat 1993). Fracturing, as well as the emplacement of basalts through discontinuous magnetic events and the common occurrence of lower crustal intrusions, makes layer 2A more heterogeneous and permeable at slow than at fast spreading centres. Consequently, layer 2A is probably altered more and thus less magnetized at slow spreading centres.

While the alteration of the upper crustal basalts results in a loss of magnetization, the alteration of lower crustal and uppermost mantle peridotites more than likely transforms these rocks into serpentinites and produces magnetite, resulting in the acquisition of new magnetization (see Toft, Arkani-Hamed & Haggerty 1990 for a further description of serpentinization). Harrison (1987) suggests that as much as 16 per cent of layer 3 may consist of serpentinite. Assuming serpentinization to begin below 530 °C (Wooldrige *et al.* 1990) or at about 350 °C (Krammer 1990; Nazarova 1994), the thermal evolution of the oceanic lithosphere shows that serpentinized material of the lower crust and uppermost mantle may significantly contribute to the sea-floor spreading magnetic anomalies. Owing to tectonics, intrusives and discontinuous magmatic processes, the oceanic crust at slow spreading centres is more permeable and allows more vigourous and deeper hydrothermal circulations. Peridotites at slow spreading ridges should be more rapidly and more pervasively serpentinized, allowing a consistent NRM pattern to be acquired by the lower crust and uppermost mantle. The uppermost mantle is richer in peridotite than layer 3, and serpentinization is expected to produce more magnetization in the uppermost mantle. However, the increasing difficulty that hydrothermal fluids have in reaching the uppermost mantle, due to increasing lithostatic pressure and decreasing permeability and fracturing with depth, may hamper, to some extent, serpentinization of the uppermost mantle. In addition, low magma supply at slow spreading centres results in diapiric intrusion of peridotites into the gabbroic lower crust (Cannat 1993). This increases the amount of peridotites, and therefore the production of magnetite through serpentinization, in the lower crust of slow/cool spreading centres.

Many combinations of these effects may contribute to the spreading-rate-dependent magnetization of the oceanic lithosphere. Slow spreading centres are characterized by low fractionated and highly altered basaltic crust, and numerous intrusive and serpentinized peridotites in the lower crust, resulting in a relatively weaker layer 2A magnetization and a relatively stronger layer 3 and uppermost mantle magnetization. On the other hand, the fast spreading centres have a basaltic crust produced by a more fractionated upper mantle, which is probably less altered, and the lower crustal peridotites are less serpentinized. Layer 2A is most likely to be the main source of magnetic anomalies at these spreading centres.

While we have provided plausible explanations for a spreading-rate-dependent magnetization of the oceanic lithosphere, the cause of the transition between anomalies with and without anomalous skewness observed at about 50 km Myr^{-1} (Dyment *et al.* 1994; Fig. 1) remains obscure. This transition does not seem to correspond to the transition between slow and fast spreading centres observed at 30–35 km Myr^{-1} on the bathymetric, gravity and seismic data and interpreted in terms of the thermal state of lithosphere, the crustal rheology and the mechanism of isostatic compensation. We suggest that the magnetic transition between marine magnetic anomalies with a significant anomalous skewness and those with negligible anomalous skewness is related to the percolation of hydrothermal fluids through the upper crust (e.g. Guéguen, David & Gavrilenko 1991). At low percolation, the fluids do not pervasively penetrate into the lower crust and serpentinization only exists locally, whereas at higher percolation hydrothermal fluids reach the lower crust and cause pervasive serpentinization. This suggestion is based on the premise that the permeability of the upper crust varies with spreading rate, in agreement with a crust that is more heterogeneous and fractured at slow spreading rates than at fast ones.

Additional constraints on the variation of the layer 2A and the lower crust magnetization with spreading rate can come from direct measurements of magnetization on rock samples. However, the gabbros sampled by dredging or drilling have been tectonically transported to the surface. They may have been altered and may not be representative of the whole layer 3. Moreover, reliable measurements are too sparse to allow a systematic study of the variations of layer 3 magnetization with spreading rate.

On the other hand, a greater number of measurements of the magnetic properties of basalts recovered by drilling at DSDP and ODP sites are available. We use the 72 natural remanent magnetization (NRM) measurements compiled by Johnson & Pariso (1993) and estimate the spreading rate for each site using the digital age map (Müller *et al.* 1993) and the isochron map (Cande *et al.* 1989) of the oceans. The variation of magnetization intensity with age observed by Bleil & Petersen (1983), Furuta (1993), and Johnson & Pariso (1993) may obscure possible variations with spreading

rate: measurements on oceanic crust younger than 25 Ma show a fast decay of magnetization with age related to the rapid alteration of the young oceanic basalts, whereas those on oceanic crust older than 75 Ma show an increase of magnetization with age. Fig. 3 shows the measured NRM intensities (corrected for palaeolatitude effect and reduced to the Equator) versus spreading rate for three different age groups: younger than 25 Ma (40 values), 25–75 Ma (14 values), and older than 75 Ma (18 values). The small number of measurements within each group and their uneven distribution with spreading rate preclude any meaningful statistical analysis, so these data are only examined qualitatively. Fig. 3(b) shows the lowest NRM intensities, as expected. This diagram is consistent with a constant layer 2A maximum magnetization of 3 A m^{-1} if we ignore the high NRM measurement at 90 km Myr^{-1} (dashed line), and with a linear increase of layer 2A maximum magnetization from 2.5 A m^{-1} at 5 km Myr^{-1} to 7 A m^{-1} at 90 km Myr^{-1} if we consider this measurement (solid line). Fig. 3(c) displays strong NRM intensities that apparently decrease with faster spreading rate. A more careful analysis, however, reveals that this trend (and possibly the increase of magnetization observed for NRM intensity versus age) may be related to some regional bias, as all of the high intensities at slow spreading rate indeed come from the western Central Atlantic Ocean (from an area limited by 10°N–30°N and 280°E–305°E). Two other high NRM intensity measurements, at sites 256 and 260 in the eastern Indian Ocean, are, respectively, dated 101 Ma and 107 Ma, a period characterized by the nearby emplacement of the huge volcanic Kerguelen Plateau–Broken Ridge structure (Whitechurch *et al.* 1992). Older basalts from the same area show much lower NRM intensities (Johnson & Pariso 1993). The NRM intensity measurements for oceanic crust older than 75 Ma are locally affected by the intensive mid-Cretaceous volcanism associated, for instance, with the formation of numerous oceanic plateaus (Larson 1991). The remaining NRM intensity measurements for oceanic crust older than 75 Ma (i.e. excluding the western Central Atlantic and sites 256 and 260, 8 values) are consistent with the trends defined from the age 25–75 Ma (Figs 3c and d). Fig. 3(a) shows stronger values, as alteration is still in progress to reduce their magnetization. Sites located in the vicinity of the Galapagos Islands have anomalously high NRM values, in agreement with the high-amplitude magnetic anomalies observed in the area (e.g. Vogt 1979), which reflect a possible effect of the Galapagos hotspot. If these sites are

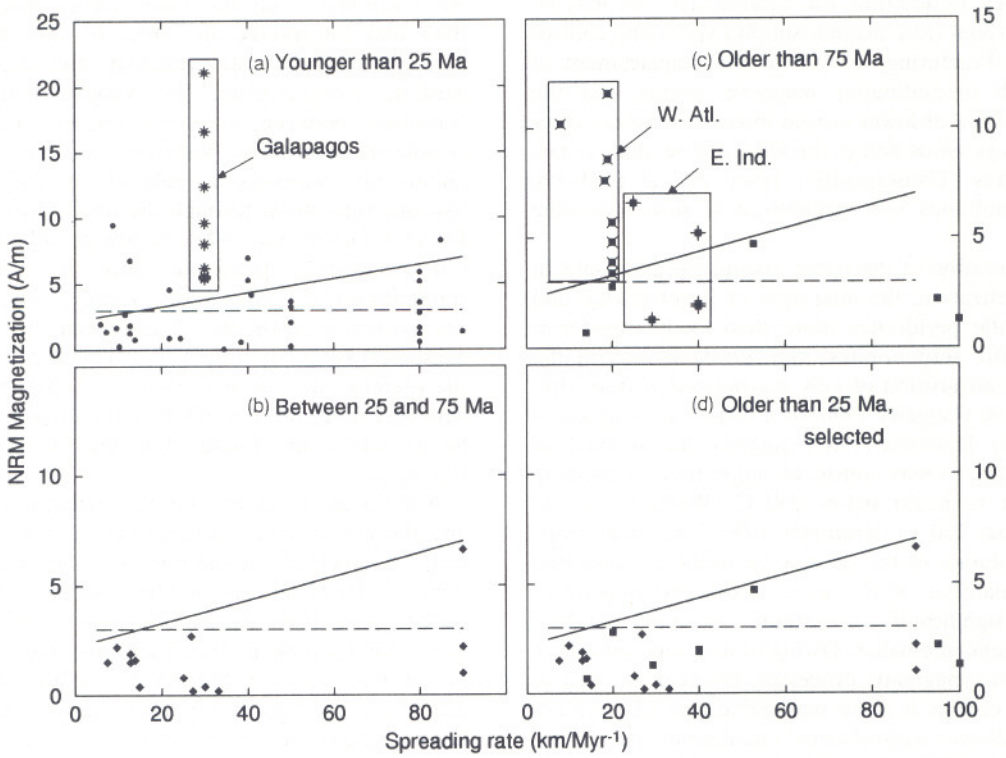

Figure 3. Natural remanent magnetization (NRM) intensity of oceanic basalts (Johnson & Pariso 1993) versus spreading rate. Three time intervals are considered: younger than 25 Ma (a), 25–75 Ma (b), and older than 75 Ma (c), to avoid the effect of age-dependent variations. Data from the Galapagos area, the western Central Atlantic and eastern Indian Oceans are shown by superposition of '*', '×', and '+', respectively. The data acquired in the vicinity of an active hotspot (Galapagos, some of the Indian Ocean measurements) are not considered. In addition, western Central Atlantic data on basalts older than 75 Ma show a clear regional bias, and are also not considered. The measured NRMs were possibly acquired under varying geomagnetic polarities. We tentatively define the maximum magnetization, i.e., the magnetization that would have been acquired under a constant geomagnetic polarity, as the upper bound of the measured NRMs. Both a constant maximum magnetization of 3 A m^{-1} (dashed line) and an increasing maximum magnetization with increasing spreading rate between 2.5 A m^{-1} at 5 km Myr^{-1} and 7 A m^{-1} at 90 km Myr^{-1} (solid line) are consistent with the NRM measurements between 25 and 75 Ma (b), the selected measurements older than 25 Ma (d), and to a lesser extent with those younger than 25 Ma (a).

excluded, NRM intensities are consistent with both (but do not permit discrimination between) a constant and a linearly increasing maximum magnetization with spreading rate.

Magnetization model of the oceanic lithosphere

The TRM–VRM model of the crust and uppermost mantle used in this study is a modified version of Arkani-Hamed's (1989) model. This model is built on the basis of a typical thermal evolution model of the oceanic lithosphere. Acquisition of TRM is simulated for magnetic materials with a range of magnetic blocking temperatures. A range of 400–600 °C, suitable for magnetite, was adopted for the lower crust and uppermost mantle, as magnetite is probably the main magnetic mineral in gabbros and serpentinites (e.g. Pariso & Johnson 1993a). A range of 200–400 °C, which is more representative of titanomagnetites, is adopted for the basaltic layer 2A. However, the rapid cooling of the upper crust makes the choice of this blocking temperature range of secondary importance, as the boundaries between opposite polarities are essentially vertical and narrow in this part of the crust (Arkani-Hamed 1990).

Considering the uncertainties about its contribution to magnetic anomalies, a zero magnetization is assigned to layer 2B in all of the models presented in this paper. Due to fast cooling, this layer can have a magnetic pattern similar to that of layer 2A, i.e. with almost vertical and narrow transition zones between opposite polarities, as has been observed in ophiolites (e.g. Kidd 1977). If layer 2B has some contribution to the sea-floor spreading anomalies, the magnetization we assigned to layer 2A includes this contribution.

Arkani-Hamed (1989) restricted the acquisition of viscous magnetization to the first 0.1 Myr after a geomagnatic field reversal, because of computer limitations. We have developed a better approach, based on the equation (Richter 1937; Dunlop 1973, 1983)

$$M(t) = M_\infty(1 - e^{-t/\tau}) + M_0 e^{-t/\tau}, \quad (1)$$

in which $M(t)$ is the magnetization at time t after a reversal, M_∞ is the saturation magnetization, M_0 is the initial magnetization immediately after the reversal and τ is the characteristic relaxation time of magnetization, which depends on temperature among other parameters. For single-domain magnetic materials, Pullaiah *et al.* (1975) proposed the relation

$$T_1/k(T_1)\log(f_0\tau_1) = T_2/k(T_1)\log(f_0\tau_2), \quad (2)$$

in which τ_i is the blocking temperature, τ_i is the relaxation time, $f_0 \sim 10^{10}\,s^{-1}$ is the characteristic frequency of thermal fluctuations, and $k(T_i) \sim [J_s(T_i)]^2$ for magnetite, J_s being the spontaneous magnetization. Walton (1981) suggested another relation,

$$[T_1/k(T_1)]^{2+r}[\log(f_0\tau_1)]^{3+r} = [T_2/k(T_2)]^{2+r}[\log(f_0\tau_2)]^{3+r}, \quad (3)$$

and proposed $r = -1$ (log-normal distribution) or $r = -1.6$ (agreement with experiment). Our simulations show that Walton's (1981) approach predicts more viscous magnetization than does Pullaiah *et al.*'s (1975), leads to a complete removal of TRM for a 200–400 °C blocking temperature range, and implies that the upper crust mainly bears viscous magnetization. It is therefore clearly inadequate to produce the observed sea-floor spreading magnetic anomalies. Moreover, Walton's (1981) model was criticized on the basis of theoretical argument by Worm & Jackson (1988). Therefore we adopt Pullaiah *et al.*'s (1975) relationship. Also, we assume that the decay of magnetization due to alteration observed during the first 20 to 30 Myr of the formation of the oceanic crust has already taken place because our skewness measurements come from anomalies older than 40 Myr.

Using the TRM–VRM model of the crust and uppermost mantle as a premise, we investigate the variations of magnetization of layer 2A, layer 3 and the uppermost mantle with spreading rate required to explain the observed relationship between the anomalous skewness and the spreading rate. Following Arkani-Hamed's (1989) convention, we call $m1$, $m3$ and $m4$ the saturation magnetizations of layer 2A, layer 3 and uppermost mantle, respectively. Rather than the amount of magnetization of layers, the ratios of magnetization between layers ($m3/m1$ and $m4/m1$) are the parameters that control the anomalous skewness. We do not expect to obtain a reliable constraint on the variations of the uppermost mantle magnetization, as this layer has only a small effect on magnetic anomalies at sea-level, and the anomalous skewness of Magsat anomalies associated with the Cretaceous Quiet Zone has only been measured in the North Atlantic Ocean (LaBrecque & Raymond 1985).

In the first attempt, the uppermost mantle magnetization is neglected (model 1). Fig. 4(a) shows the anomalous skewness of the synthetic anomalies 33r and 25r for different ratios of $m3/m1$ and different spreading rates. For both anomalies, the predicted anomalous skewness is almost independent of spreading rate for a low $m3/m1$ ratio, and it slightly decreases with increasing spreading rate for low to intermediate values of $m3/m1$. For anomaly 33r, the anomalous skewness increases with increasing spreading rate for high $m3/m1$ values, whereas for anomaly 25r it first increases and then decreases with increasing spreading rate. Comparison with the real measurements shows that anomaly 25r measurements are consistent with a model that has as $m3/m1$ ratio varying from 0, at and above a spreading rate of 50 km Myr^{-1}, to about 2 : 6 at 20 km Myr^{-1}. Anomaly 33r measurements, however, disagree with such a model. Since the two actual measurements at spreading rates of 7.5 and 22 km Myr^{-1}. (Roest *et al.* 1992) are above the upper bound of predicted anomalous skewness, a magnetic uppermost mantle is required to account for the observed anomalous skewness.

Within the framework of the TRM–VRM model of the crust and uppermost mantle, the anomalous skewness of marine magnetic anomalies is mainly controlled by the magnetization of layer 3 (Arkani-Hamed 1989). Therefore we next examine a model that has layer 2A and uppermost mantle magnetizations independent of spreading rate and an $m4/m1$ ratio of 1 : 4, whereas layer 3 magnetization is assumed to vary with spreading rate (model 2). The predicted anomalous skewness is found to be similar to that of model 1.

Model 3 assumes that layer 3 and the uppermost mantle

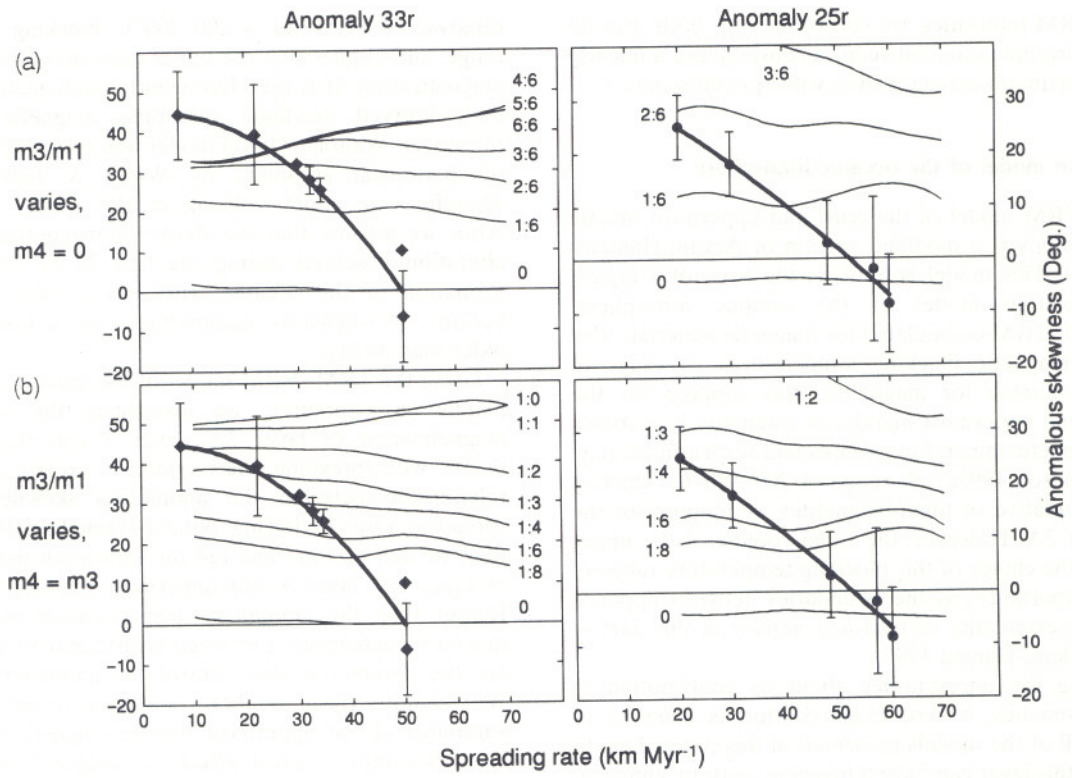

Figure 4. (a) Anomalous skewness predicted for anomalies 33r (left) and 25r (right) by a magnetization model with magnetic blocking temperature ranging between 400 and 600 °C and various ratios of layer 3 to layer 2A magnetizations. Magnetization is equal to 0 in layer 2B (depth of 0.5 to 2.5 km) and in the uppermost mantle (below a depth of 7 km). Observed anomalous skewness is also shown (symbols as in Fig. 2). (b) As (a), but with uppermost mantle magnetization equal to layer 3 magnetization.

have the same amount of saturation magnetization ($m3 = m4$). Because of the slower decrease of temperature, it takes a considerable length of time for the uppermost mantle to cool through the magnetic blocking temperature. During this long period, the core field polarity changes several times, producing partial thermoremanent magnetization of opposite polarities. Also, the viscous magnetization is significant at higher temperatures of the uppermost mantle. Therefore, the resulting magnetization of the uppermost mantle is actually much weaker than that of the lower crust and the actual base of the layer bearing a significant magnetization is about 10 km, much shallower than the 30 km maximum depth that we allow in our computations. This model investigates the relative variations of layer 2A magnetization on the one hand and layer 3 and the uppermost mantle magnetization on the other. One end member of this class of models assumes that only the magnetization of layer 2A varies with spreading rate, and another end member considers a spreading-rate-dependent magnetization of layer 3 and uppermost mantle while that of layer 2A is independent of spreading rate. For instance, the curves labelled by the $m3/m1$ ratios 1 : 0 to 1 : 8 (Fig. 4a,b) are computed for layer 2A magnetization ranging from 0 to 12 A m^{-1} and a constant $m3 = m4 = 1.5$ A m^{-1}. The upper bound for anomaly 33r allows the observed skewness for a slow spreading rate to be properly modelled. Skewness measurements for fast spreading rates, close to zero, require that $m3$ and $m4$ decrease to 0 A m^{-1}, corresponding to the curve labelled 0 in Fig. 4(b).

For models 1 ($m4 = 0$), 2 ($m4/m1 = 1 : 4$), and 3 ($m4 = m3$), we determined the $m3/m1$ ratios required to satisfy anomaly 33r and 25r measurements by picking the intersections of synthetic and observed anomalous skewness versus spreading rate curves in Fig. 4, the observed data being fitted by a smooth curve. The results are displayed in Figs 5(a), (b) and (c), respectively. Models 1 and 2 do not explain the spreading-rate dependence of anomalous skewness measured on anomalies 33r and 25r with similar $m3/m1$ variations; the curves of $m3/m1$ versus spreading rate are divergent at slow spreading rates, and a consistent $m3/m1$ value cannot be obtained for spreading rates slower than 30 km Myr^{-1} (model 1) or 20 km Myr^{-1} (model 2). On the contrary, the curves of $m3/m1$ versus spreading rate for model 3 are rather similar for both anomaly 33r and 25r measurements, considering the large uncertainties associated with the measurements (see Fig. 4). This model defines a linear trend between an $m3/m1$ of 0.4 at a spreading rate of 10 km Myr^{-1} and 0 at 55 km Myr^{-1} (Fig. 5c). Modifications of this model by changing the $m4/m3$ ratio from 1 to 2 : 3 (model 4) and to 4 : 3 (model 5) do not result in significant improvements to the match of anomaly 33r and 25r curves (Figs 5d and e). Model 4 leads to results similar to those of models 1 and 2 and thus is not suitable, whereas model 5 yields a fit of anomaly 33r and 25r curves similar to or even slightly better than that of Model 3. The increasing discrepancy with decreasing spreading rates is more than likely related to the larger error of the anomalous skewness measurements at slow spreading rates.

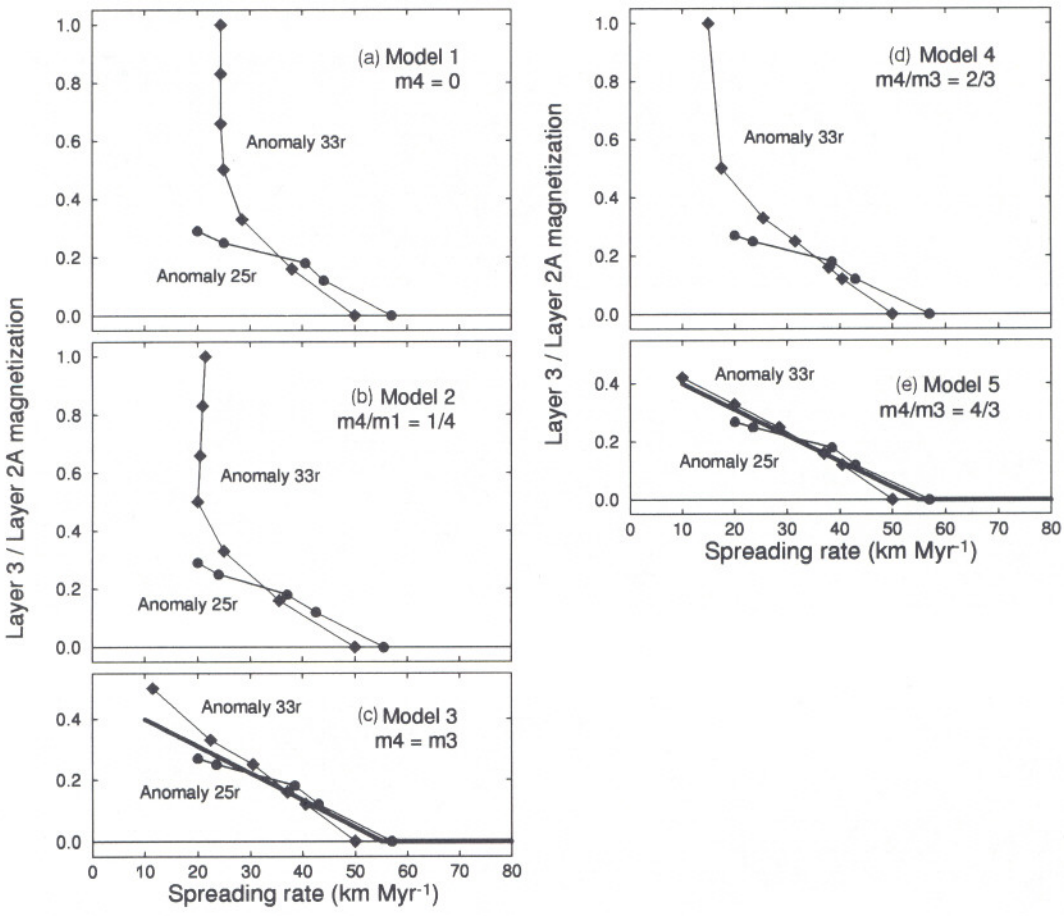

Figure 5. Ratio of layer 3 to layer 2A magnetizations required to satisfy anomalous skewness measurements on anomalies 33r (diamond) and 25r (circles) versus spreading rate for model 1 (no upper mantle magnetization), model 2 (uppermost mantle saturation magnetization is 1 : 4 of that of layer 2A), model 3 (uppermost mantle saturation magnetization is equal to that of layer 3), model 4 (uppermost mantle saturation magnetization is 2 : 3 of that of layer 3), and model 5 (uppermost mantle saturation magnetization is 4 : 3 of that of layer 3). Models 1, 2 and 4 show diverging curves for anomalies 33r and 25r, and are rejected. The thick line for models 3 and 5 shows possible variations of the ratio of layer 3 to layer 2A saturation magnetizations with spreading rate.

Based on the above extensive exercise, we propose the following model for the magnetization of the oceanic lithosphere: (1) layer 3 and the uppermost mantle bear a similar saturation magnetization, $m3 = m4$; and (2) the $m3/m1$ ratio decreases linearly with the spreading rate, V, as

$$\begin{aligned} m3/m1 &= -0.009V + 0.49 \qquad 10 < \mathrm{V} < 50\ \mathrm{km\ Myr^{-1}}, \\ m3/m1 &= 0 \qquad\qquad\qquad\quad \mathrm{V} > 50\ \mathrm{km\ Myr^{-1}}. \end{aligned} \tag{4}$$

It should be noted that the anomalous skewness constrains the $m1/m3$ ratio but not the intensity of $m1$ and $m3$.

The NRM intensity measurements of basalts do not provide a strong constraint on the variations of $m1$ with spreading rate. We consider two magnetization models for layer 2A, a constant magnetization of $6\ \mathrm{A\ m^{-1}}$, and a spreading-rate-dependent magnetization varying linearly from $3\ \mathrm{A\ m^{-1}}$ at a spreading rate of $10\ \mathrm{km\ Myr^{-1}}$ to $6\ \mathrm{A\ m^{-1}}$ at $55\ \mathrm{km\ Myr^{-1}}$. Fig. 6 displays the magnetization pattern of the second model for spreading rates of 10, 35 and $60\ \mathrm{km\ Myr^{-1}}$. At each spreading rate, layer 2A bears the strongest magnetization. At intermediate and slow spreading rates, the magnetization pattern of the lower crust and uppermost mantle display characteristic 'tails' away from the spreading centre, which are responsible for the anomalous skewness. Although they have the same saturation magnetization, the actual magnetization of the uppermost mantle is much less than that of the lower crust, due to slow cooling during which the core field polarity changes frequently and reduces the resulting magnetization, and also due to the increasing effect of viscous magnetization with depth. Fig. 7 shows the magnetic anomalies 20 to 34 (45 to 85 Ma), computed at the pole (top) and phase-shifted to de-skew anomaly 33r (middle) and anomaly 25r (bottom) for both models and for selected spreading rates. The skewness factors obtained for anomalies 33r and 25r are in agreement with the observations (see Fig. 1). The major difference between the anomalies predicted by the two models is the amplitude of the de-skewed anomalies. For the first model, the amplitude at slow spreading rate is about twice the amplitude at fast spreading rate. For the second model, the amplitude is almost independent of the spreading rate. The second model seems more realistic, although no detailed quantitative analysis of the variations of marine magnetic anomaly

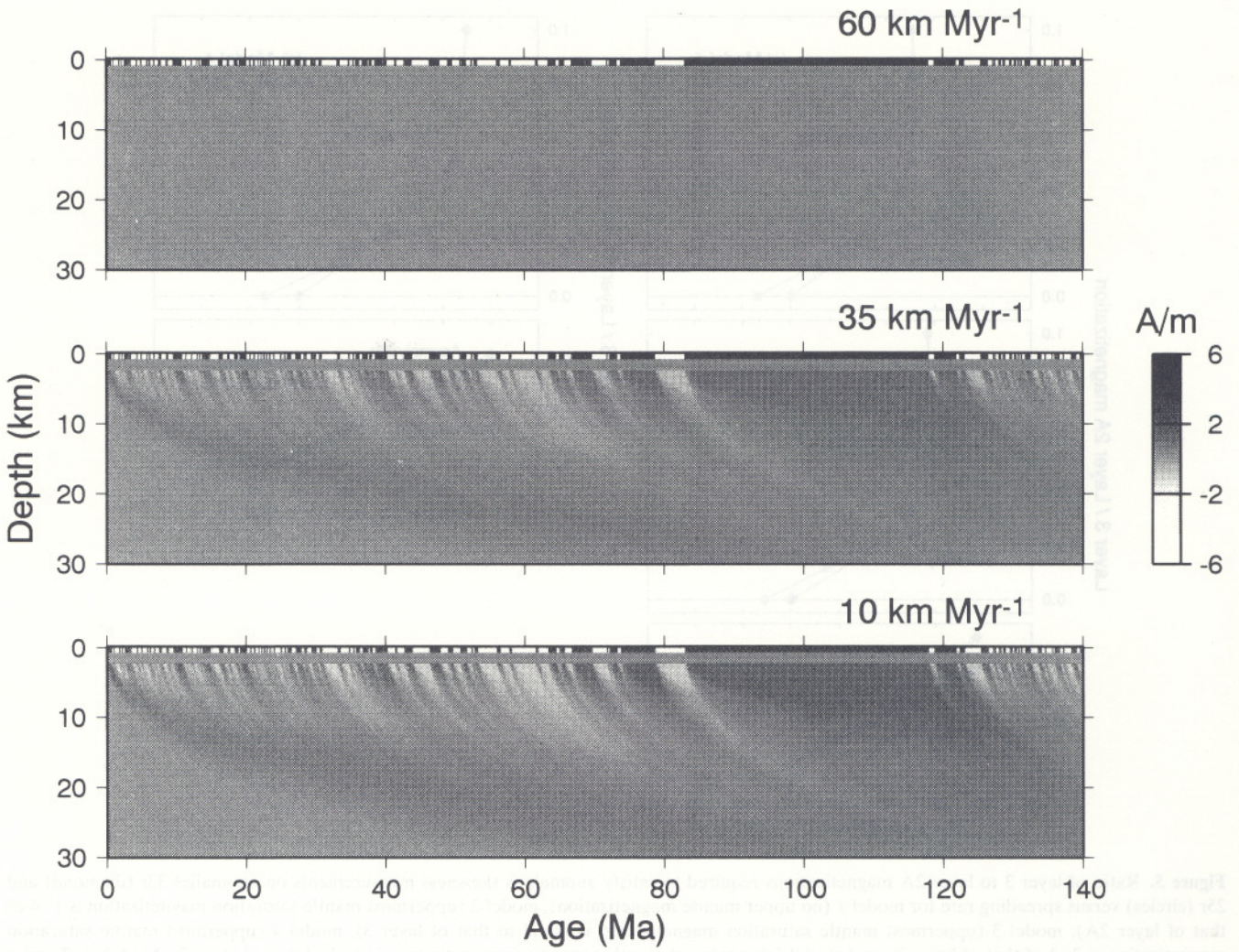

Figure 6. Distribution of magnetization in oceanic lithosphere for constant spreading rates of 60, 35 and 10 km Myr^{-1} (from top to bottom). Layer 2A magnetization is equal to 6 A m^{-1} at a spreading rate of 55 km Myr^{-1}, 4.5 A m^{-1} at 35 km Myr^{-1}, and 3 A m^{-1} at 10 km Myr^{-1}. Layer 2B bears no magnetization. Layer 3 and the uppermost mantle have the same saturation magnetization, while the ratio of layer 3 to layer 2A magnetizations varies as in Fig. 5, models 3 and 5.

amplitude with spreading rate is available. Such analysis, which is beyond the scope of this paper, would provide the necessary constraint to estimate the variations of $m1$ with spreading rate.

Although our model provides a satisfactory explanation for the observed anomalous skewness, it should be noted that it is built on several simplifying assumptions. For instance, the thermal evolution model does not change with spreading rate, as it should to take into account the existence/absence of a partially molten magma chamber at fast/slow spreading centres. The magnetization model does not consider any variation with spreading rate of the physical parameters of TRM and VRM acquisition (such variation is indeed poorly known), and only the intensity of saturation magnetization varies with spreading rate. No attempt is made in this paper to build a physical model of serpentinization; we are presently studying this issue. In addition, the numerical values obtained in this study, such as in relation (4), are dependent on the various thermal and magnetic input parameters, and should only be regarded as a first-order approximation. Despite these shortcomings, we believe that a spreading-rate-dependent magnetization of the oceanic layers provides a reasonable explanation for the observed anomalous skewness, does not contradict NRM intensity measurements, and is supported by current ideas on the accretionary processes at the mid-ocean ridge axis.

CONCLUSIONS

The existing magnetization models of the oceanic lithosphere used for explaining the anomalous skewness—temporal variations of the geomagnetic field, crustal tectonic rotations, alteration of primary TRM and acquisition of secondary CRM in layer 2A, and thermally controlled acquisition of TRM and VRM in the entire crust and uppermost mantle—do not successfully predict the relationship observed between the anomalous skewness and spreading rate. We propose a new model, based on the anomalous skewness of anomalies 33r and 25r, in which the magnetic structure of the oceanic lithosphere is dependent on spreading rate. In our preferred model, layer 3 and the uppermost mantle bear a similar saturation magnetization.

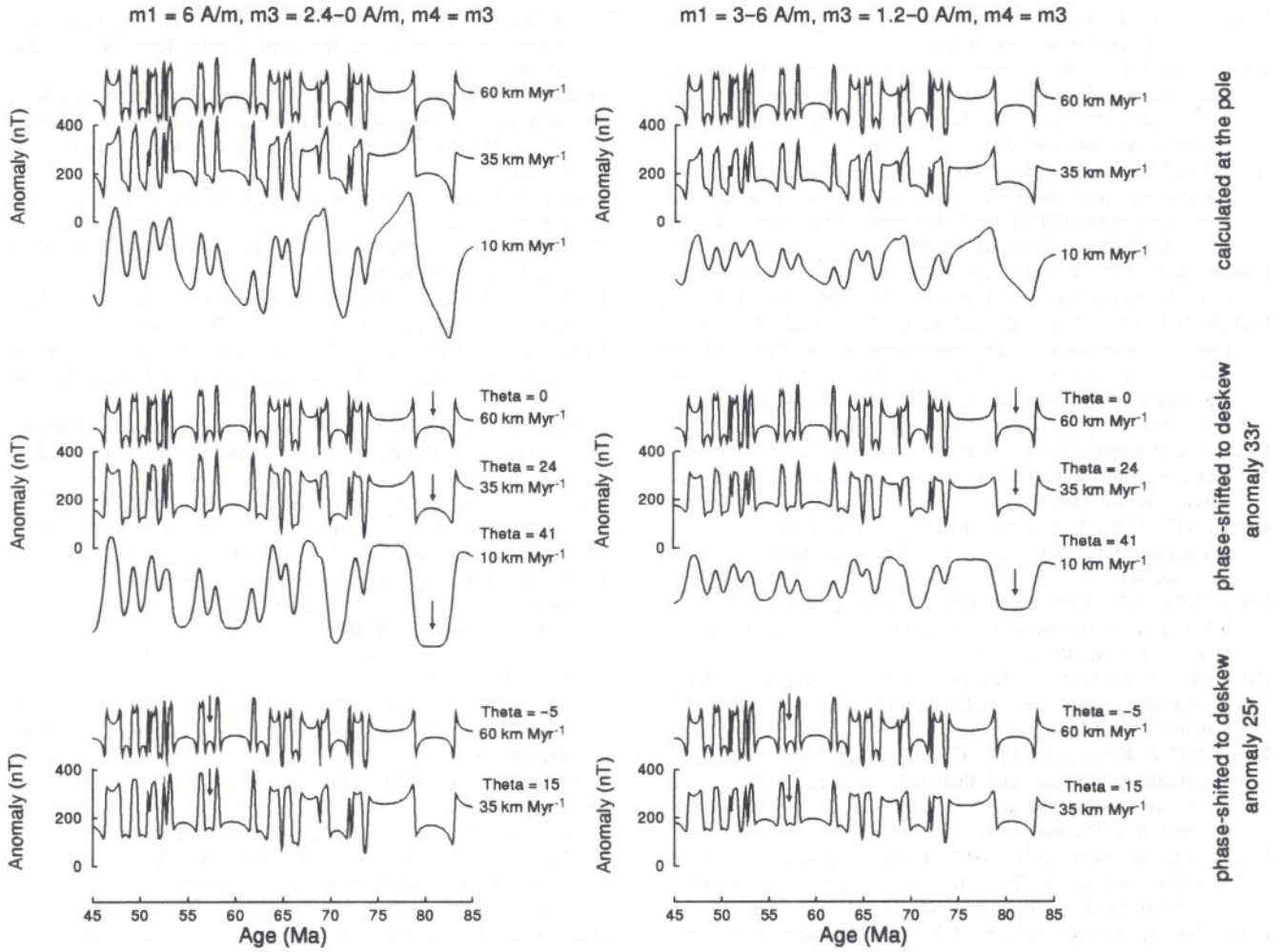

Figure 7. Magnetic anomalies 21 to 34 for constant spreading rates of 55, 35 and 10 km Myr^{-1}, for a constant (left) and varying (right, corresponds to the magnetization distributions displayed in Fig. 6) saturation magnetization of layer 2A with spreading rate. Layer 2B bears no magnetization. Layer 3 and the uppermost mantle have the same saturation magnetization, while the ratio of layer 3 to layer 2A magnetizations varies as in Fig. 5, models 3 and 5. The anomalies computed at the pole (top) were phase-shifted in order to get anomalies 33r (middle) and 25r (bottom) symmetrical. The resulting skewness factors are in agreement with the observations (see Fig. 1) for both models, which differ only by the amplitude variation with spreading rate.

The ratio of layer 3 over layer 2A saturation magnetizations varies linearly from about 0.4 at a spreading rate of 10 km Myr^{-1} to about 0 at 55 km Myr^{-1}. For spreading rates higher than 55 km Myr^{-1}, layer 3 and the uppermost mantle magnetizations are negligible. The transition at a spreading rate of about 50 km Myr^{-1}, above which there is no anomalous skewness, is probably due to the percolation of hydrothermal fluids, which controls the serpentinization of layer 3 and the uppermost mantle.

ACKNOWLEDGMENTS

This work was made possible by the award of an International Fellowship by the Natural Science and Engineering Research Council (NSERC) of Canada to JD, and was supported by NSERC Operating Grant No. OGP0041245. We thank J. L. LaBrecque and J. Verhoef for providing a copy of their programs to compute the CRM distribution in the crust, P. Wessel and W. H. F. Smith for the GMT software used to produce Fig. 6, and P. J. Turner for the Xmgr software used to produce the other figures. We acknowledge many constructive discussions with A. Ghods at McGill, comments by C. Raymond and H. Schouten on an earlier version of this manuscript, and reviews by N. Petersen and two anonymous scientists.

REFERENCES

Arkani-Hamed, J., 1989. Thermoviscous remanent magnetization of oceanic lithosphere inferred from its thermal evolution, *J. geophys. Res.*, **94,** 17 421–17 436.

Arkani-Hamed, J., 1990. Magnetization of the oceanic crust beneath the Labrador Sea, *J. geophys. Res.*, **95,** 7101–7110.

Arkani-Hamed, J., 1991. Thermoremanent magnetization of the oceanic lithosphere inferred from a thermal evolution model: implications for the source of marine magnetic anomalies, *Tectonophysics,* **192,** 81–96.

Arkani-Hamed, J. & Strangway, D.W., 1987. An interpretation of magnetic signatures of subduction zones detected by Magsat, *Tectonophysics,* **133,** 45–55.

Banerjee, S.K., 1984. The magnetic layer of the oceanic crust—how thick is it? *Tectonophysics,* **105,** 15–27.

Beske-Diehl, S.J., 1989. Comment on "Magnetization of the oceanic crust: thermoremanent magnetization or chemical remanent magnetization?" by C. A. Raymond & J. R. LaBrecque, *J. geophys. Res.,* **94,** 3046–3048.

Bina, M.M. & Henry, B., 1990. Magnetic properties, opaque mineralogy and magnetic anisotropies of serpentinized peridotites from ODP Hole 670A near the Mid-Atlantic Ridge, *Phys. Earth planet. Inter.,* **65,** 88–103.

Blakely, R.J., 1974. Geomagnetic reversals and crustal spreading rates during the Miocene, *J. geophys. Res.,* **79,** 2979–2985.

Blakely, R.J., 1976. An age-dependent, two-layer model for marine magnetic anomalies, in *The geophysics of the Pacific Ocean basin and its margin, Geophys. Monograph.,* **19,** pp. 227–234, eds Sutton, G.H., Manghnani, M.H., Moberly, R. & McAfee, E.U., Am. Geophys. Union, Washington, DC.

Bleil, U. & Petersen, N., 1983. Variations in magnetization intensity and low-temperature titanomagnetite oxidation of ocean floor basalts, *Nature,* **301,** 384–388.

Cande, S.C., 1976. A palaeomagnetic pole from Late Cretaceous marine magnetic anomalies in the Pacific, *Geophys. J. R. astr. Soc.,* **44,** 547–566.

Cande, S.C., 1978. Anomalous behavior of the paleomagnetic field inferred from the skewness of anomalies 33 and 34, *Earth planet. Sci. Lett.,* **40,** 275–286.

Cande, S.C. & Kent, D.V., 1976. Constraints imposed by the shape of marine magnetic anomalies on the magnetic source, *J. geophys. Res.,* **81,** 4157–4162.

Cande, S.C. & Kent, D.V., 1985. Comment on "Tectonic rotations in extensional regimes and their paleomagnetic consequences for ocean basalts" by K. L. Verosub & E. M. Moores, *J. geophys. Res.,* **90,** 4647–4651.

Cande, S.C. & Kent, D.V., 1992. Ultrahigh resolution marine magnetic anomaly profiles: a record of continuous paleointensity variations? *J. geophys. Res.,* **97,** 15075–15083.

Cande, S.C. & Kristoffersen, Y., 1977. Late Cretaceous magnetic anomalies in the North Atlantic, *Earth planet. Sci. Lett.,* **35,** 215–224.

Cande, S.C. & LaBrecque, J.L., 1974. Behaviour of the Earth's palaeomagnetic field from small scale marine magnetic anomalies, *Nature,* **247,** 26–28.

Cande, S.C., LaBrecque, J.L., Larson, R.L., Pitman, W.C., Golovechenko, X. & Haxby, W.F., 1989. *Magnetic lineations of the World's Ocean basins* (map), Am. Assoc. of Petroleum Geologists, Tulsa, OK.

Cannat, M., 1993. Emplacement of mantle rocks in the seafloor at mid-ocean ridges, *J. geophys. Res.,* **98,** 4163–4172.

Chen, Y.J., 1992. Ocean crustal thickness versus spreading rate, *Geophys. Res. Lett.,* **19,** 753–756.

Christensen, N.I. & Salisbury, M.H., 1972. Seafloor spreading, progressive aleration of layer 2 basalts, and associated changes in seismic velocities, *Earth planet. Sci. Lett.,* **15,** 367–375.

Cochran, J.R., 1979. An analysis of isostasy in the world's oceans, 2, Mid-ocean ridge crests, *J. geophys. Res.,* **84,** 4713–4729.

Cochran, J.R., 1991. Systematic variation of axial morphology along the Southeast Indian Ridge (abstract), *EOS Trans. Am. geophys. Un.,* **72,** 260.

Counil, J.-L., Achache, J. & Galdeano, A., 1989. Long wavelength magnetic anomalies in the Caribbean, *J. geophys. Res.,* **94,** 7419–7431.

Cox, A., 1969. Geomagnetic reversals, *Science,* **163,** 237–245.

Cox, A., 1975. The frequency of geomagnetic reversals and the symmetry of the non-dipole field, *Rev. Geophys. Space Phys.,* **13,** 35–51.

Davis, E.E. & Lister, C.R.B., 1974. Fundamentals of ridge crest topography, *Earth planet. Sci. Lett.,* **21,** 405–413.

Detrick, R.S., Bulh; P., Vera, E., Mutter, J., Orcutt, J., Madsen, J. & Brocher, T., 1987. Multichannel seismic imaging of a crustal magma chamber along the East Pacific Rise, *Nature,* **236,** 35–41.

Detrick, R.S., Mutter, J.C., Bulh, P. & Kim, I.I., 1990. No evidence from multichannel reflection data for a crustal magma chamber in the MARK area on the Mid-Atlantic Ridge, *Nature,* **347,** 61–64.

Dunlop, D.J., 1973. Theory of the magnetic viscosity of lunar and terrestrial rocks, *Rev. Geophys. Space Phys.,* **11,** 855–901.

Dunlop, D.J., 1981. The rock magnetism of fine particles, *Phys. Earth planet. Inter.,* **26,** 1–26.

Dunlop, D.J., 1983. Viscous magnetization of 0.04–100 μm magnetites, *Geophys. J. R. astr. Soc.,* **74,** 667–687.

Dunlop, D.J. & Hale, C.J., 1977. Simulation of long-term changes in the magnetic signal of the oceanic crust, *Can. J. Earth Sci.,* **14,** 716–744.

Dunlop, D.J. & Prévot, M., 1982. Magnetic properties and opaque mineralogy of drilled submarine intrusive rocks, *Geophys. J. R. astr. Soc.,* **69,** 763–802.

Dyment, J., Cande, S.C. & Arkani-Hamed, J., 1994. Skewness of marine magnetic anomalies created between 85 and 40 Ma in the Indian Ocean, *J. geophys. Res.,* **99,** 24 121–24 134.

Furuta, T., 1993. Magnetic properties and ferromagnetic mineralogy of oceanic basalts, *Geophys. J. Int.,* **113,** 95–114.

Geiss, E., Petersen, N. & Bleil, U., 1989. Amplitude variation of marine magnetic anomalies, *Geologische Rundschau,* **78,** 741–752.

Guéguen, Y., David, C. & Gavrilenko, P., 1991. Percolation networks and fluid transport in the crust, *Geophys. Res. Lett.,* **18,** 931–934.

Harrison, C.G.A., 1976. Magnetization of the oceanic crust, *Geophys. J. R. astr. Soc.,* **47,** 257–283.

Harrison, C.G.A., 1981. Magnetism of the oceanic crust, in *The sea,* **7,** pp. 219–239, ed. Emiliani, C., Wiley, New York.

Harrison, C.G.A., 1987. Marine magnetic anomalies—the origin of the stripes, *Annu. Rev. Earth planet. Sci.,* **15,** 505–543.

Harrison, C.G.A. & Carle, H.M., 1981. Intermediate wavelength magnetic anomalies over oceanic basins, *J. geophys. Res.,* **86,** 11585–11599.

Hayling, K.L., 1991. Magnetic anomalies at satellite altitude over continent–ocean boundaries, *Tectonophysics,* **192,** 129–143.

Huang, P.Y. & Solomon, S.C., 1988. Centroid depths of mid-ocean ridge earthquakes: dependence on spreading rate, *J. geophys. Res.,* **93,** 13 445–13 477.

Johnson, H.P. & Pariso, J.E., 1993. Variations in oceanic crustal magnetization: systematic changes in the last 160 million years, *J. geophys. Res.,* **98,** 435–445.

Kent, D.V., Honnorez, B.M., Opdyke, N.D. & Fox, P.J., 1978. Marine properties of dredged oceanic gabbros and the source of marine magnetic anomalies, *Geophys. J. R. astr. Soc.,* **55,** 513–537.

Kidd, R.G.W., 1977. The nature and shape of the sources of marine magnetic anomalies, *Earth planet. Sci. Lett.,* **33,** 310–320.

Klein, E.M. & Langmuir, C.H., 1989. Local versus global variation in ocean ridge basaltic composition: a reply, *J. geophys. Res.,* **94,** 4241–4252.

Krammer, K., 1990. Rock magnetic properties and opaque mineralogy of selected samples from Hole 670A, *Proc. ODP Sci. Results,* **106/109,** 269–273.

LaBrecque, J.L. & Raymond, C.A., 1985. Seafloor spreading anomalies in the Magsat field of the North Atlantic, *J. geophys. Res.,* **90,** 2565–2575.

Larson, R.L., 1991. Latest pulse of the Earth: evidence for a mid-Cretaceous superplume, *Geology,* **19,** 547–550.

Levi, S., 1979. Paleomagnetism and some magnetic properties of basalts from the Bermuda triangle, in *Initial Reports of the DSDP,* **51-52-53** Part 2, pp. 1363–1378, eds. Donelly, T. *et al.,* US Government Printing Office, Washington, DC.

Macdonald, K.C., 1977. Near-bottom magnetic anomalies, asymmetric spreading, oblique spreading, and tectonics of the Mid-Atlantic Ridge near lat 37°N, *Geol. Soc. Am. Bull.*, **88,** 541–555.

Macdonald, K.C., 1982. Mid-ocean ridges: fine scale tectonic, volcanic, and hydrothermal processes within the plate boundary zone, *Ann. Rev. Earth planet. Sci.*, **10,** 155–190.

Macdonald, K.C., 1986. The crest of the Mid-Atlantic Ridge: models for crustal generation processes and tectonics, in *The geology of North America*, **M,** *The western North Atlantic Region,* pp. 51–68, eds Vogt, P.R. & Tucholke, B.E., Geol. Soc. of America, Boulder, CO.

Macdonald, K.C. & Luyendyk, B.P., 1977. Deep-tow studies of the structure of the Mid-Atlantic Ridge crest near lat. 37°N, *Geol. Soc. Am. Bull.*, **88,** 621–636.

Macdonald, K.C. & Luyendyk, B.P., 1985. Investigation of faulting and abyssal hill formation on the flanks of the East Pacific Rise (21°N), using Alvin, *Mar. Geophys. Res.*, **7,** 515–535.

Macdonald, K.C., Miller, S.P., Luyendyk, B.P., Atwater, T.M. & Shure, L., 1983. Investigation of a Vine–Matthews magnetic lineation from a submersible: the source and character of marine magnetic anomalies, *J. geophys. Res.*, **88,** 3403–3418.

Malinverno, A., 1991. Inverse square-root dependence of mid-ocean-ridge flank roughness on spreading rate, *Nature,* **352,** 58–60.

Malinverno, A., 1993. Transition between a valley and a high at the axis of mid-ocean ridges, *Geology*, **21,** 639–642.

McKenzie, D.P., 1969. Speculations on the consequences and causes of plate motions, *Geophys. J. R. astr. Soc.*, **18,** 1–32.

Morton, J.L. & Sleep, N.H., 1985. Seismic reflections from a Lau Basin magma chamber, in *Geology and offshore resources of Pacific Islands arcs—Tonga region, Earth Sci. Ser.*, **2,** pp. 441–453, eds Scholl, D.W. & Vallier, T.L., Circum-Pacific Council for Energy and Mineral Resources, Houston, TX.

Morton, J.L., Sleep, N.H., Normark, W.R. & Tomkins, D.H., 1987. Structure of the southern Juan de Fuca Ridge from seismic reflection records, *J. geophys. Res.*, **92,** 11 315–11 326.

Müller, R.D., Roest, W.R., Royer, J.Y., Gahagan, L.M. & Sclater, J.G., 1993. *A digital age map of the ocean floor,* file available by anonymous ftp from baltica.ucsd.edu, directory pub/global–age.

Nazarova, K.A., 1994. Serpentinized peridotites as a possible source for oceanic magnetic anomalies, *Mar. Geophys. Res.*, **16,** 455–462.

Niu, Y. & Batiza, R., 1993. Chemical variation trends at fast and slow spreading mid-ocean ridges, *J. geophys. Res.*, **98,** 7887–7902.

Pariso, J.E. & Johnson, H.P., 1993a. Do lower crustal rocks record reversals of the Earth magnetic field? Magnetic petrology of oceanic gabbros from ODP Hole 735B, *J. geophys. Res.*, **98,** 16 013–16 032.

Pariso, J.E. & Johnson, H.P., 1993b. Do layer 3 rocks make a significant contribution to marine magnetic anomalies? In situ magnetization of gabbros at Ocean Drilling Program Hole 735B, *J. geophys. Res.*, **98,** 16 033–16 052.

Parmentier, E.M. & Phipps Margon, J., 1990. Spreading rate dependence of three-dimensional structure in oceanic spreading centres, *Nature*, **348,** 325–328.

Petronotis, K.E., Gordon, R.G. & Acton, G.D., 1989. Paleomagnetic poles with a fine time resolution: a chron 25 (56.5–57.5 Ma) Pacific plate pole determined from shape analysis of marine magnetic anomalies (abstract), *EOS Trans. Am geophys. Un.*, **70,** 1064

Phillips, J.D. & Cox, A., 1976. Spectral analysis of geomagnetic reversal time scales, *Geophys. J. R. astr. Soc.*, **43,** 19–33.

Phillips, J.D., Blakely, R.J. & Cox, A., 1975. Independence of geomagnetic polarity intervals, *Geophys. J. R. astr. Soc.*, **43,** 747–754.

Pozzi, J.P. & Dubuisson, G., 1992. High temperature viscous magnetization of oceanic deep crustal and mantle rocks as a partial source for Magsat magnetic anomalies, *Geophys. Res. Lett.*, **19,** 21–34.

Pullaiah, G., Irving, E., Buchan, K.L. & Dunlop, D.J., 1975. Magnetization changes caused by burial and uplift, *Earth planet. Sci, Lett.*, **28,** 133–143.

Purdy, G.M., Kong, L.S.L., Christeson, G.L. & Solomon, S.C., 1992. Relationship between spreading rate and the seismic structure of mid-ocean ridges, *Nature*, **355,** , 815–817.

Raymond, C.A. & LaBrecque, J.L., 1987. Magnetization of the oceanic crust: thermoremanent magnetization or chemical remanent magnetization? *J. geophys. Res.*, **92,** 8077–8088.

Reid, I. & Jackson, H.R., 1981. Oceanic spreading rate and crustal thickness, *Mar. Geophys. Res.*, **5,** 165–172.

Richter, G., 1937. Über die magnetische Nachwirkung am Carbonyleisen, *Ann. Physik*, **29,** 605–635.

Roest, W.R., Arkani-Hamed, J. & Verhoef, J., 1992. The sea-floor spreading rate dependence of the anomalous skewness of marine magnetic anomalies, *Geophys. J. Int.*, **109,** 653–669.

Sauter, D., Whitechurch, H., Munschy, M. & Humler, E., 1991. Periodicity in the accretion on the Southeast Indian Ridge at 27°40′ S, *Tectonophysics*, **195,** 47–64.

Sayanagi, K. & Tamaki, K., 1992. Long-term variations in magnetization intensity with crustal age in the northeast Pacific, Atlantic, and southeast Indian oceans, *Geophys. Res. Lett.*, **19,** 2369–2372.

Schouten, H. & McCamy, K., 1972. Filtering marine magnetic anomalies, *J. geophys. Res.*, **77,** 7089–7099.

Sempere, J.C., 1991. High-magnetization zones near spreading center discontinuities, *Earth Planet. Sci. Lett.*, **107,** 389–405.

Sinton, J.M. & Detrick, R.S., 1992. Mid-ocean ridge magma chambers, *J. geophys. Res.*, **97,** 197–216.

Sleep, N.H., 1975. Formation of oceanic crust: some thermal constraints, *J. geophys. Res.*, **80,** 4037–4042.

Small, C. & Sandwell, D.T., 1989. An abrupt change in ridge axis gravity with spreading rate, *J. geophys. Res.*, **94,** 17 383–17 392.

Small, C. & Sandwell, D.T., 1992. An analysis of ridge axis gravity roughness and spreading rate, *J. geophys. Res.*, **97,** 3235–3245.

Smith, B.M., 1984. Magnetic Viscosity of some doleritic basalts in relation to the interpretation of the oceanic magnetic anomalies, *Geophys. Res. Lett.*, **11,** 213–216.

Smith, G.M., 1985. Source of marine magnetic anomalies: some results from DSDP Leg 83, *Geology*, **13,** 162–165.

Smith, G.M. & Banerjee, S.K., 1986. Magnetic structure of the upper kilometer of the marine crust at Deep Sea Drilling Project Hole 504B, eastern Pacific Ocean, *J. geophys. Res.*, **91,** 10 337–10 354.

Spudich, P. & Orcutt, J., 1980. A new look at the seismic velocity structure of the oceanic crust, *Rev. Geophys. Space Phys.*, **18,** 627–658.

Stein, C.A. & Stein, S., 1994. Constraints on hydrothermal heat flux through the oceanic lithosphere from global heat flow, *J. geophys. Res.*, **99,** 3081–3095.

Tauxe, L., 1993. Sedimentary records of relative paleointensity of the geomagnetic field: theory and practice, *Rev. Geophys.*, **31,** 319–354.

Toft, P.B. & Arkani-Hamed, J., 1992. Magnetization of the Pacific Ocean lithosphere deduced from Magsat data, *J. geophys. Res.*, **97,** 4387–4406.

Toft, P.B., Arkani-Hamed, J. & Haggerty, S.E., 1990. The effects of serpentinization on density and magnetic susceptibility: a petrophysical model, *Phys. Earth planet. Inter.*, **65,** 137–157.

Valet, J.P. & Meynadier, L., 1993. Geomagnetic field intensity and reversals during the past four million years, *Nature,* **366,** 234–238.

Verhoef, J. & Arkani-Hamed, J., 1990. Chemical remanent

magnetization of oceanic crust, *Geophys. Res. Lett.*, **17,** 1945–1948.

Verosub, K.L. & Moores, E.M., 1981. Tectonic rotations in extensional regimes and their paleomagnetic consequences for oceanic crust, *J. geophys. Res*, **86,** 6335–6349.

Vogt, P.R., 1979. Amplitude of oceanic magnetic anomalies and the chemistry of oceanic crust: synthesis and review of 'magnetic telechemistry', *Can. J. Earth Sci.*, **16,** 2236–2262.

Walton, D., 1981. Time–temperature relations in the magnetization of assemblies of single domain grains, *Nature,* **286,** 245–247.

Whitechurch, H., Montigny, R., Sevigny, J., Storey, M. & Salters, V., 1992. K–Ar and ^{40}Ar–^{39}Ar ages of central Kerguelen Plateau basalts, *Proc. Ocean Drill. Program Sci. Results,* **120,** 71–77.

Wittpenn, N.A., Harrison, C.G.A. & Handschumacher, D.W., 1989. Crustal magnetization in the South Atlantic from inversion of magnetic anomalies, *J. geophys. Res.,* **94,** 15 463–15 480.

Wooldridge, A.L., Haggerty, S.E., Rona, P.A. & Harrison, C.G.A., 1990. Magnetic properties and opaque mineralogy of rocks from selected seafloor hydrothermal sites at oceanic ridges, *J. geophys. Res.*, **95,** 12 351–12 374.

Worm, H.Y. & Jackson, M., 1988. Theoretical time–temperature relationships of magnetization for distributions of single domain magnetite grains, *Geophys. Res. Lett.*, **15,** 1093–1096.